Sheffield Hallam University

Biological and structural studies of phosphonium 'masked thiolate' compounds

CHEN, Yu-Su, ALLEN, David, CROSS, Neil A <http://orcid.org/0000-0003-2055-5815>, PITAK, Mateusz B, TIZZARD, Graham J, COLES, Simon J and BRICKLEBANK, Neil <http://orcid.org/0000-0002-1614-2260>

Citation:

Research paper

Biological and structural studies of phosphonium 'masked thiolate' compounds

Yu-Su Chen [a], David W. Allen [a], Graham J. Tizzard [b], Mateusz B. Pitak [b], Simon J. Coles [b], Neil A. Cross [a, *], Neil Bricklebank [a, *]

[a] Biomolecular Sciences Research Centre, Sheffield Hallam University, Sheffield S1 1WB, UK
[b] UK National Crystallography Service, Chemistry, Highfield Campus, Southampton SO17 1BJ, UK

ABSTRACT

The ability of phosphonium cations to act as intracellular transport vectors is well-established. Phosphonioalkylthiosulfate zwitterions, and ω-thioacetylalkylphosphonium salts, which act as 'masked thiolate' ligands, are useful precursors for the formation of phosphonium-functionalised gold nanoparticles, enabling the nanoparticles to be transported into cells for diagnostic and therapeutic purposes. In this study we have completed cytotoxicity studies of ω-thioacetylpropylphosphonium salts derived from triphenylphosphine and tri(4-fluorophenyl)phosphine, which show that the compounds are only toxic towards PC3 prostate cancer cells at high concentrations and at prolonged incubation periods and display IC_{50} values of 67 μM and 252 μM respectively, significantly higher than those of other phosphonium salts. MALDI-TOF-MS has been used to investigate the uptake of the compounds by PC3 cells and to quantify detectable levels of the compounds inside the cells. The structures of ω-thioacetylpropyl(tri-4-fluorophenyl) phosphonium bromide and the corresponding tri(4-fluorophenyl)phosphoniopropylthiosulfate zwitterion have been investigated by single crystal X-ray crystallography. The results show that molecules of the zwitterion are held together through an extensive array of electrostatic and non-covalent interactions. The unit cell of ω-thioacetylpropyl(tri-4-fluorophenyl)phosphonium bromide contains eight cations together with eight bromide anions and two waters of crystallisation, all held together through a complex network of hydrogen bonds. The differences in the molecular packing of the two compounds may account for the lower solubility of the zwitterion in aqueous solutions, compared with that of the phosphonium salt.

© 2016 The Authors. Published by Elsevier Masson SAS. This is an open access article under the CC BY-NC-ND license (http://creativecommons.org/licenses/by-nc-nd/4.0/).

1. Introduction

Phosphonium compounds are versatile species that find application in diverse fields ranging from synthetic reagents, *e.g.*, in the Wittig reaction, to flame retardant materials and ionic liquids. A remarkable feature of phosphonium compounds is their ability to cross cell membranes and be concentrated inside mitochondria without the need for a transporter protein or chaperone [1].

In recent years, it has become evident that mitochondrial dysfunction contributes to a range of human diseases, including cancer and neurodegenerative disorders, and there has been an increase in effort made towards the development of pharmacological strategies which can transport molecules into this organelle [2]. Consequently, phosphonium groups have been conjugated to a wide variety of species including metal complexes [3], dendrimers [4], liposomes [5] and nanoparticles [6–8], with a view to their potential applications in mitochondria-targeted diagnostics and therapeutics.
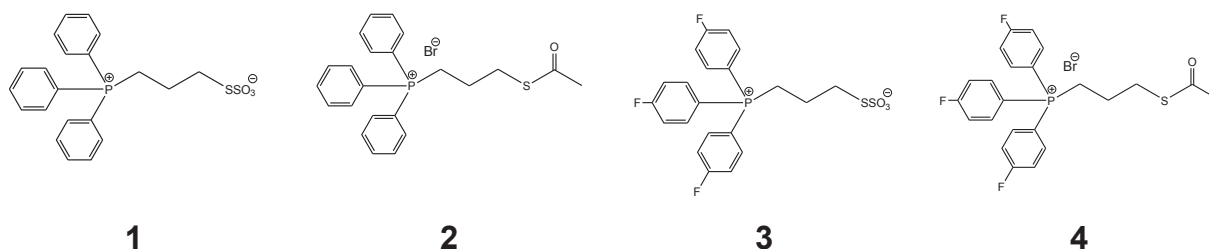
Previously we have prepared a series of phosphonioalkylthiosulfate zwitterions [9], and ω-thioacetylalkylphosphonium salts [10], which act as 'masked thiolate' ligands; under reductive conditions, the thiosulfate and thioacetate groups cleave, generating phosphonioalkylthiolate anions that can attach to the surface of gold nanoparticles, generating phosphonioalkylthiolate-functionalised gold nanoparticles [7,8]. The phosphonium-functionalised gold nanoparticles can be isolated and are readily taken-up by the mitochondria of cancer cells [8,11].

It has been demonstrated that the rate and extent of uptake of phosphonium compounds *in vitro* are affected by the hydrophobicity of the compound [12]. The addition of fluorine has been routinely applied in medicinal chemistry to modify the physiochemical properties of drugs; fluorine has been incorporated into compounds to improve metabolic stability, lipophilicity and binding affinity with an

overall target to increase the bioavailability of the product [13]. Furthermore phosphonium compounds labelled with radioactive ^{18}F have been developed as a new class of lipophilic positron emission tomography (PET) radiotracers [14]. As part of our investigations into the chemistry and biology of phosphonium compounds and phosphonium-functionalised nanomaterials, we report herein the cellular-uptake and cytotoxicity data for the ω-thio-acetylalkylphosphonium derivatives of triphenyl- and 4-fluorophenyl-phosphine together with structural investigations of the tri(4-fluorororophenyl)phosphoniopropyl thiosulfate zwitterion and ω-thioacetylalkyl(tri-4-fluorophenyl)phosphonium bromide salt.

spectrometry (MALDI-TOF-MS) is a widely used analytical tool due to its high-speed analysis, simplicity and excellent sensitivity. Although MALDI-TOF-MS has transformed the analysis of large biomolecules, its application to small molecules with molar masses typically below 1000 Da has lagged behind. Demand for high-throughput methods in drug discovery and biotechnology has driven the utilisation of MALDI-TOF-MS in small molecule analysis [16]. There are two reports on the use of MALDI-TOF-MS to quantify the uptake of phosphonium compounds in cells. Rideout and colleagues were the first to demonstrate the quantitative analysis of phosphonium cations by MALDI-TOF-MS, showing that
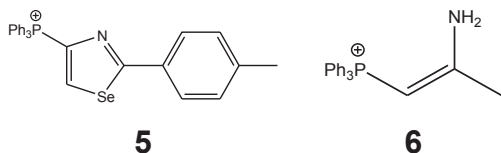
1   **2**   **3**   **4**

2. Results

2.1. Cytotoxicity of phosphonioalkyl-thiosulfate zwitterions and -thioacetate salts

Preliminary investigations into the cytotoxicity of **1**–**4** indicated that the thiosulfate zwitterions, **1** and **3**, are non-toxic. The thio-sulfate zwitterions are only sparingly soluble in water, DMSO, methanol and biological media; however, thioacetate salts **2** and **4** are soluble in aqueous solvent systems and we have been able to determine the cellular uptake and cell viability of these compounds.

The cytotoxicity of compounds **2** and **4** against the PC3 prostate cell cancer line was determined using the CellTitre-Glo® assay, which uses luminescence to determine the number of viable cells based on a quantification of ATP levels. The data are presented in Fig. 1. The data show that compounds **2** and **4** are only toxic towards PC3 cells at high concentrations and at prolonged incubation periods, with calculated IC_{50} values of 67 μM and 252 μM for **2** and **4**, respectively, at 72 hours. The IC_{50} values reported here are significantly higher than those of other phosphonium-containing molecules. Millard and co-workers have determined the cytotoxicity of 33 phosphonium compounds, all containing the triphenylphosphonium moiety linked to different chemical groups, in five different cell lines [15]. Their most toxic compound, TP 731 (**5**), has an IC_{50} in PC3 cells of 0.4 μM at 72 h, *ca.*160-fold more toxic than **2**, whilst the least toxic compound TP 764 (**6**) has an IC_{50} of 8 μM at 72 h, which is still 16-fold more toxic than **2**, indicating that the ω-thioacetylpropyltriphenylphosphonium salts investigated in this study are comparatively non-toxic towards cells.

5   **6**

2.2. Use of MALDI-TOF-MS to study the uptake of ω-thioacetylalkylphosphonium salts by PC3 cancer cells

Matrix-assisted laser desorption/ionisation time-of-flight mass
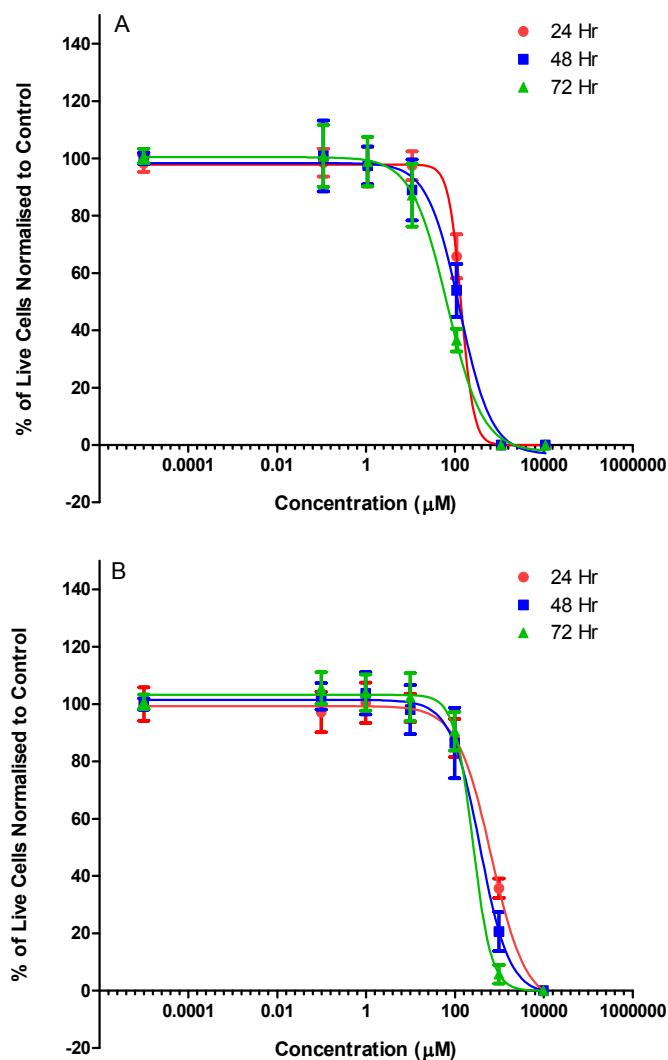

Fig. 1. PC3 cells treated with ω-thioacetylalkylphosphonium salts (a) **2**, and (b) **4**, for 24, 48 and 72 h. Cell proliferation was determined by the CellTiter-Glo™ luminescent cell viability assay kit. Data are expressed as a percentage of live cells normalised to control, mean ± SD (n = 12).

tetraphenylphosphonium salts were taken-up in sub-femtomole amounts in carcinoma cell lines [17]. Cheng and co-workers reported the uptake of a range of phosphonium cations in the sub-femtomole region by C6 rat glioma cells using MALDI-TOF-MS [18]. In MALDI experiments, a matrix is incorporated into the sample preparation stage to provide efficient desorption and soft ionisation of the analyte. The previous studies of phosphonium compounds in cells used α−CHCA (α-cyano-4-hydroxycinnamic acid) as the matrix, the most common matrix used for the analysis of small molecules [16]. However, α−CHCA was unsuitable for the analysis of **2** because the molecular ion peak [M]$^+$ is at m/z 379 which coincides with the α−CHCA dimer peak [2 M + H]$^+$ at m/z 379. This presented a problem for quantification work, as the peak area would be either under- or over-estimated making the results unreliable. Consequently DHB (2,5-dihydroxybenzoic acid), which is the other matrix commonly used for the analysis of small organic molecules [16], was employed for the analysis of **2**. In order to improve experimental reproducibility, an internal standard is usually employed for the MALDI analysis of lower molecular weight molecules. In this study tetraphenylphosphonium bromide was used because of its chemical similarity to **2** and **4**; Fig. 2 shows the ion intensity ratio of the product ion m/z 379 and m/z 433 for **2** and **4**, respectively, against [Ph$_4$P]Br at m/z 339. The calibration curves (Fig. 3) demonstrate that the ion intensity ratio increases with increasing concentration of **2** and **4**. The MALDI-TOF-MS spectra in Fig. 4 show the ion intensities of **2** at m/z 379 and the internal standard at m/z 339 at each incubation time point. Similar data were obtained for **4,** confirming that these ω-thio-acetylalkylphosphonium salts are readily taken-up by cells. The up-take of **2** and **4** as a function of time is illustrated in Fig. 5 and shows that the compounds exhibit different uptake profiles. Compound **2** is rapidly taken-up by the cells, reaching a maximum uptake at 10 min, which then drops slightly, reaching a plateau after 30 min. In contrast, **4** reaches a maximum uptake three times slower than that of **2** before declining and reaching a plateau after 90 min. Similar differences have been noted in the up-take and accumulation of tetraphenylphosphonium and 4-fluorophenyl(triphenyl)phosphonium cations by C6 glioma cells [18].

2.3. Structural studies of the tri(4-fluororophenyl) phosphoniopropyl thiosulfate zwitterion (3) and the ω-thioacetylpropyl(tri-4-fluorophenyl)phosphonium bromide salt (4)

Given the differences in the solubility of the phosphoniumalkylthiosulfate zwitterions compared to the thioacetate salts, and the differences in the IC$_{50}$ and cellular up-take of thioacetate derivatives **2** and **4**, we decided to investigate the crystal structures of the tri(4-fluorophenyl)phosphonium compounds **3** and **4**. The structures of few other organic thiosulfate zwitterions have been described in the literature. We have previously reported the structure of **1**, together with that of the tributylphosphoniothiosulfate zwitterion (**7**) [9]. The only other crystallographically characterised thiosulfate zwitterions are the ammonium derivative S-[4-(trimethylammonio)phenyl]thiosulfate (**8**) [19], and the triphenylarsoniopropyl thiosulfate zwitterion [20].
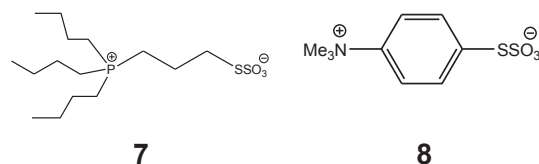
Single crystals of **3** and **4** were grown by slow diffusion of diethyl ether into dichloromethane solutions of each compound, resulting in the formation of colourless crystals. The molecular structure of **3** is shown in Fig. 6 and selected bond lengths and angles in Table 1. Zwitterion **3** displays the expected tetrahedral geometry around the phosphorus atoms with a mean C−P−C bond angle of 109.46(2)°. The corresponding values for the triphenyl and tributyl analogues **1** and **7** are 109.47(11)° and 109.47(17)°

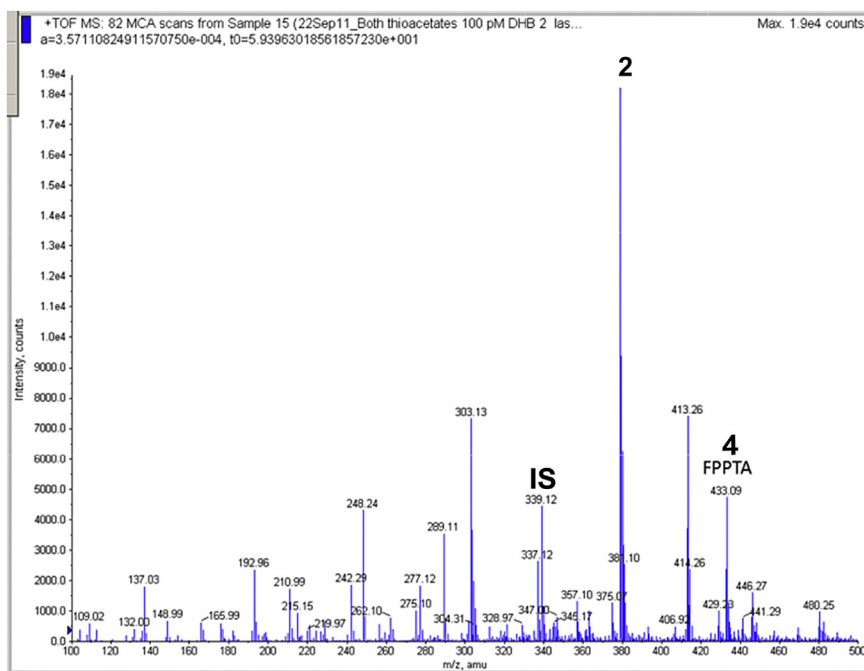**Fig. 2.** MALDI-TOF-MS spectrum of the internal standard [Ph$_4$P]Br (**IS**), **2** and **4** at the same concentration of 100 μM. Peaks noted correspond to[Ph$_4$P]Br at m/z 339.12, **2** [M]$^+$ at m/z 379.12,and **4** [M]$^+$ at m/z 433.09.
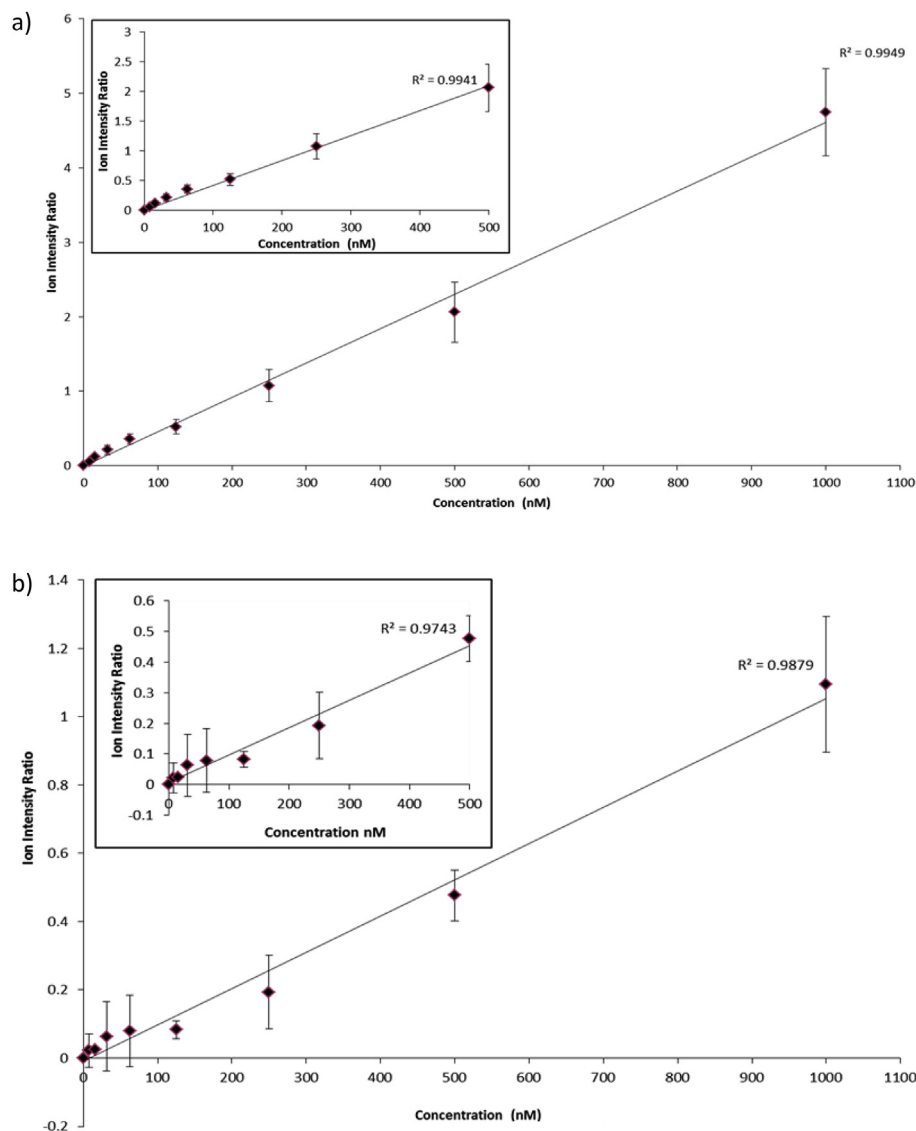
Fig. 3. MALDI-TOF-MS Calibration curve for ω-thioacetylalkylphosphonium salts (a) **2**, and (b) **4**. The graph shows that between 0 and 1000 nM, compounds **2** and **4** have a linear response of $R^2 = 0.9949$ and 0.9879 respectively. The insert in each graph shows the expanded region between 0 and 500 nM for each compound.

respectively. The bond lengths and angles in the aryl rings are unremarkable and the C–F bonds [mean length 1.361(6) Å] are similar to those in the parent phosphine, $(4\text{-}FC_6H_4)_3P$ [mean length 1.366(6) Å] [21].

The S–O bonds in the thiosulfate group of compound **3** are all similar, with a mean length of 1.439(4)Å [*c.f.* 1.4478(19) Å in **1** and 1.440(3) Å in **7**], indicative of multiple bond character. The mean O–S–O angle [113.5(3)°] is consistent with those in other thiosulfate ions. The S–S bond length [2.1076(19)Å], is slightly shorter than that of **1** [2.1117(9) Å], and longer than that in **7** [2.1030(14) Å], but all are longer than the established length of a single S–S bond [2.05 Å] [22]. The ammonium thiosulfate zwitterion **8** has an S–S bond length of 2.1137(7) Å, similar to those of **1,3** and **7**, but all are appreciably shorter than the S–S bond in the monoanion of thiosulfuric acid, $HSSO_3^-$ [2.155] [23]. The lengthening of the S–O and S–S bonds in the zwitterions is consistent with the delocalisation of the negative charge across the entire thiosulfate group. Furthermore, the longer and weaker S–S bond of the phosphonium zwitterions expedites the dissociation of the thiosulfate group with the concomitant formation of the corresponding thiolate ion which

is a key step in the application of these compounds in the synthesis of metal nanoparticles.

Within the crystal lattice the zwitterions are held together in a head-to-tail manner, by hydrogen-bonding interactions between the sulfate oxygens and the phenyl hydrogens (Fig. 7). Analysis of the supramolecular structure reveals face-to-face phenyl embrace interactions between aryl groups on adjacent molecules [24]. The centroid-centroid distance between these two rings is 3.65 Å which fits well with the interplanar spacing observed in stacked arenes which lie in the range between 3.6 and 3.8 Å [25]. The molecules also display intramolecular C–F···.H hydrogen bonding interactions between adjacent aryl rings, with an F···H distance of 2.409 Å. The nature of C–F···H interactions is the subject of some debate [26,27]. Nonetheless, the interactions in **3** are shorter than the sum of the van der Waals radii for hydrogen and fluorine (2.67 Å) and are similar in length to those found in other fluorine-containing organic molecules [27].

The molecular structure of ω-thioacetylpropyl(tri-4-fluorophenyl)phosphonium bromide **4** is shown in Fig. 8 and selected bond lengths and angles in Table 2. The asymmetric unit
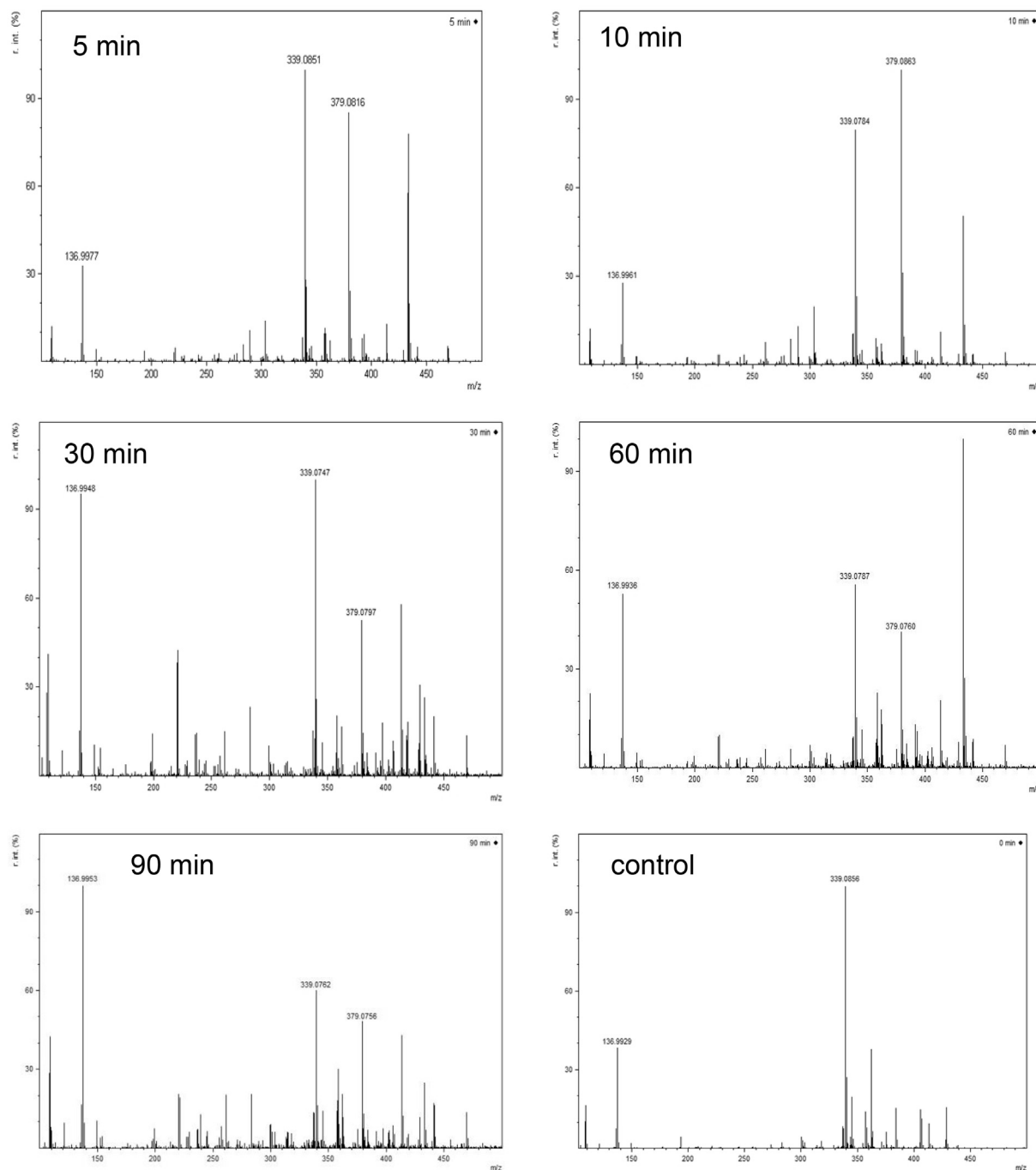
Fig. 4. Representative MALDI-TOF-MS spectra for time course of uptake of **2** in PC3 cells. PC3 cells were treated with 5 μM **2** and incubated for 5–90 min. Peaks corresponding to [M]$^+$ of **2** at m/z 379, the matrix α-CHCA at m/z 136.99 and internal standard at m/z 339.01 were observed. The control sample was PC 3 cells, internal standard and matrix alone. No [M]$^+$ peak for **2** was observed in the control which confirmed the absence of this compound in the untreated sample.

contains two crystallographically independent phosphonium cations, two bromide anions and two molecules of water of crystallisation. The bond lengths and angles of the two cations within the unit cell are very similar and lie within the normal range. The compound displays the expected tetrahedral geometry around the phosphorus atom with a mean bond angle of 109.47(3)°, identical to that in zwitterion **3**. The C–F bonds in the phenyl rings lie in the range 1.352(6) - 1.371(5), similar to those in **3** and those in the parent phosphine, which have an average length of 1.366(6) Å [21].

The C–S and C–O bond lengths of the thioacetate group in **4** are similar to the expected distances for C–S single and C=O bonds, *ca.*1.8 Å and 1.2 Å respectively [22], and are similar to the comparable bonds in ω-thioacetylpropyl(triphenyl)arsonium bromide [which has C–S bond lengths of 1.806(3)Å, 1.777(3) Å and a C=O bond length of 1.204(3) Å] [20]. Similarly, dimethylmonothiocarbonate, $CH_3OC(S)CH_3$, has C–S bond lengths of 1.791(2)Å, 1.759(1) Å and a C=O bond length of 1.195(2) Å [28].

The molecular packing displays some interesting features (Fig. 9); the unit cell contains eight cations together with eight bromide anions and water molecules which are associated with the
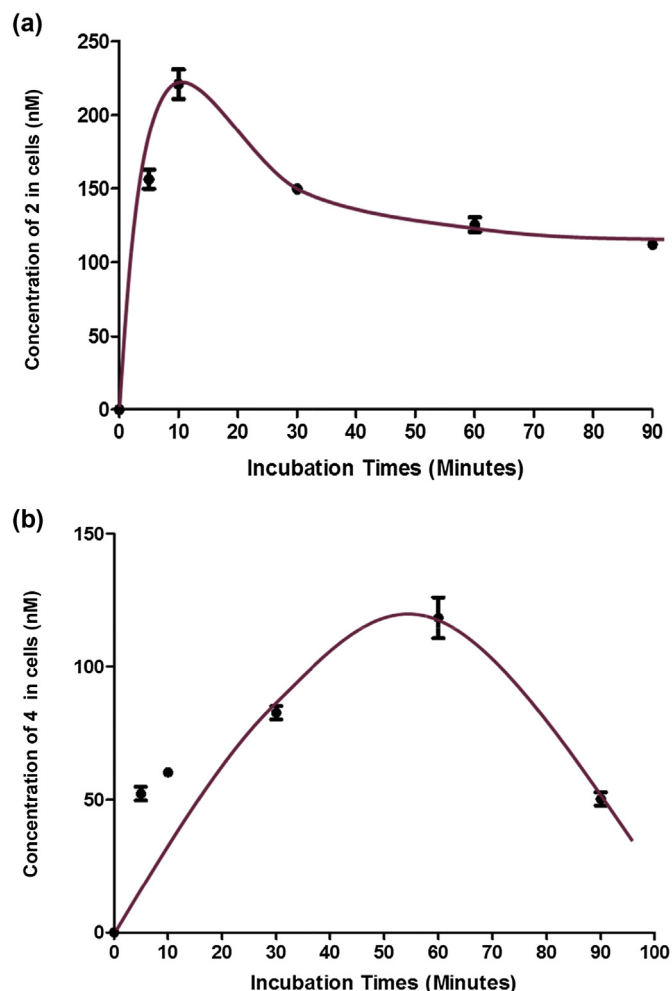
(a)

(b)

Fig. 5. The uptake and accumulation of (a) **2** and (b) **4** by PC3 cells as a function of time; PC3 cells were treated with 5 μM **2** or **4** and incubated between 0 and 90 min. Concentrations were determined from the calibration curve. Each sample was analysed in triplicate from three independent experiments.

bromide ions, all held together through a complex network of hydrogen bonds (Fig. 10) and intermolecular interactions between the different species. The structural parameters for the principal hydrogen bond interactions are presented in Table 3. The cations also display intramolecular C–F⋯.H interactions which lie in the range 2.639–2.670 Å. These distances are slightly longer than those observed in zwitterion **3**, and are close to the sum of the van der Waals radii of fluorine and hydrogen (2.67 Å), but are comparable with the distances observed in other organofluorine compounds.

3. Discussion

There is growing interest in the use of phosphonium compounds as a means of transporting a range of molecular and macromolecular and nanoscale materials into cells for diagnostic and therapeutic applications. Phosphonioalkylthiosulfate zwitterions and ω-thioacetylalkylphosphonium salts have been shown to be useful precursors for the synthesis of phosphonium-functionalised gold nanoparticles. The data reported here provide an insight into the biological behaviour of the zwitterions and salts themselves. The IC$_{50}$ values of ω-thioacetylalkylphosphonium salts **2** and **4** show the compounds to have low cytotoxicity compared to other phosphonium salts.
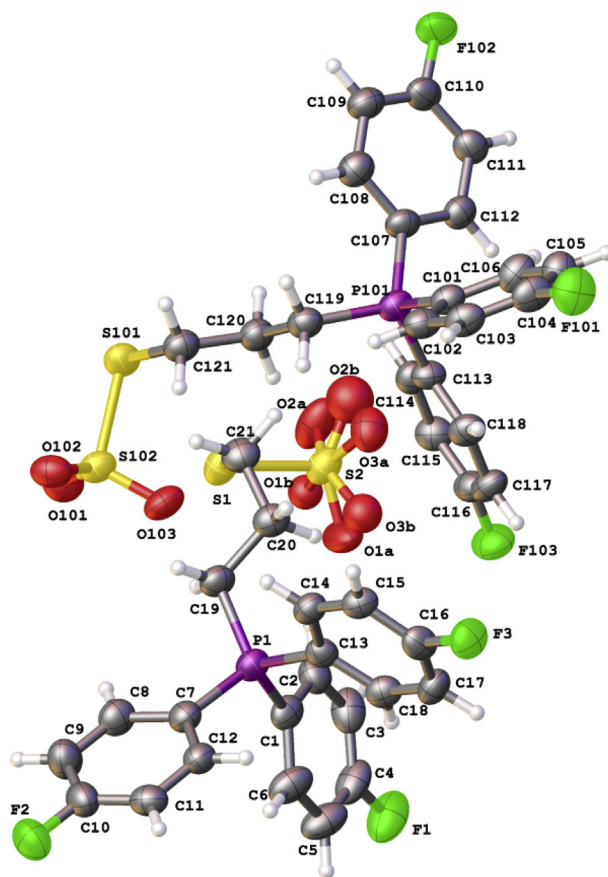

Fig. 6. Ortep representation of the molecular structure of **3**. Thermal ellipsoids are drawn at 50% probability level.

Table 1
Selected Bond Lengths (Å) and angles (°) in **3**.

P1–C1	1.794(5)	P101–C101	1.791(5)
P1–C7	1.785(5)	P101–C107	1.788(5)
P1–C13	1.798(5)	P101–C113	1.784(5)
P1–C19	1.803(4)	P101–C119	1.792(5)
S1–C21	1.808(5)	S101–C121	1.824(5)
S1–S2	2.1221(19)	S101–S102	2.0930(18)
S2–O1a	1.394(4)	S102–O101	1.442(3)
S2–O2a	1.436(4)	S102–O102	1.444(3)
S2–O3a	1.468(4)	S102–O103	1.447(3)
C1–P1–C7	109.0(2)	C101–P101–C107	108.3(2)
C1–P1–C13	109.2(2)	C101–P101–C113	109.5(2)
C1–P1–C19	110.3(2)	C101–P101–C119	109.9(2)
C7–P1–C13	107.5(2)	C107–P101–C113	108.9(2)
C7–P1–C19	110.0(2)	C107–P101–C119	110.4(2)
C13–P1–C19	110.7(2)	C113–P101–C119	109.8(2)
C20–C19–P1	114.6(3)	C120–C119–P101	114.0(3)
C20–C21–S1	114.6(3)	C120–C121–S101	115.5(3)
C21–S1–S2	101.88(19)	C121–S101–S102	100.27(17)
O1a-S2–O2a	116.6(3)	O101–S102–O102	113.9(2)
O1a-S2–O3a	113.3(3)	O101–S102–O103	114.9(2)
O2a-S2–O3a	110.1(3)	O102–S102–O103	112.2(2)
O1a-S2–S1	107.1(2)	O101–S102–S101	101.24(15)
O2a-S2–S1	103.23(19)	O102–S102–S101	106.94(15)
O3a-S2–S1	105.41(18)	O103–S102–S101	106.58(17)

A notable feature is the difference in the IC$_{50}$ values of **2** and **4**, 67 μM and 252 μM respectively after 72 hours. The only difference between the two compounds is the replacement of hydrogen in the *para* position of the phenyl rings with fluorine. This slight
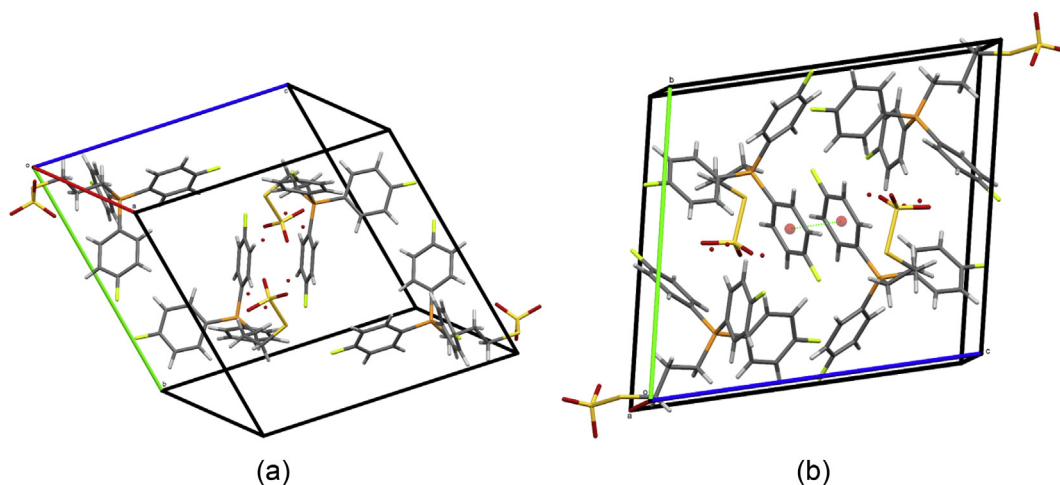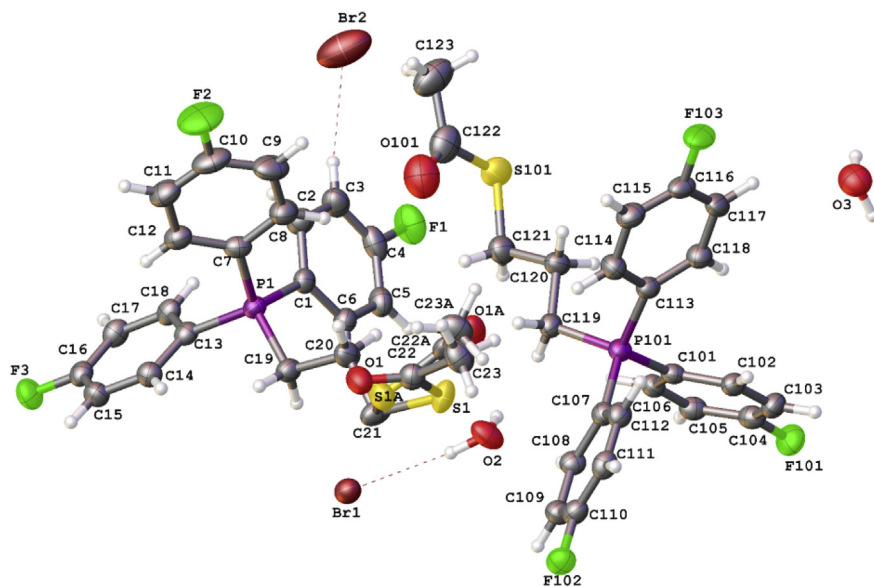
Fig. 7. (a) Molecular packing in **3** and (b) with the interaction between adjacent phenyl rings highlighted. The distance between the centres of the phenyl rings is 3.65 Å.

Fig. 8. Ortep representation of the molecular structure of **4**. Thermal ellipsoids are drawn at 50% probability level.

Table 2
Selected Bond Lengths (Å) and angles (°) in **4**.

P1–C1	1.783(5)	P101–C101	1.790(5)
P1–C7	1.792(5)	P101–C107	1.796(5)
P1–C13	1.788(5)	P101–C113	1.802(5)
P1–C19	1.808 (4)	P101–C119	1.804(5)
S1–C21	1.793(5)	S101–C121	1.794(5)
S1–C22	1.771(5)	S101–C122	1.767(7)
S1a–C21a	1.689(15)		
S1a–C22a	1.762(17)		
C4–F1	1.364(6)	C104–F011	1.359(6)
C10–F2	1.352(6)	C110–F102	1.363(5)
C16–F3	1.357(6)	C116–F103	1.371(5)
O1–C22	1.193(7)	O101–C122	1.211(8)
O1a–C22a	1.197(17)		
C1–P1–C7	109.8(2)	C101–P101–C107	108.2(2)
C1–P1–C13	109.2(2)	C101–P101–C113	111.8(2)
C1–P1–C19	109.8(2)	C101–P101–C119	110.4(2)
C7–P1–C13	109.3(2)	C107–P101–C113	111.1(2)
C7–P1–C19	110.9(2)	C107–P101–C119	108.3(2)
C13–P1–C19	107.7(2)	C113–P101–C119	107.0(2)
C21–S1–C22	100.5(3)	C121–S011–C122	101.3(3)
C21–S1a–C22a	110.8(9)		

Fig. 9. Molecular packing in **4**.

modification has a dramatic effect on the cytotoxicity of these compounds in cells. This suggests that the toxicity of these compounds is primarily determined by the phosphonium cation itself rather than by the alkylthioacetate group. This observation is in
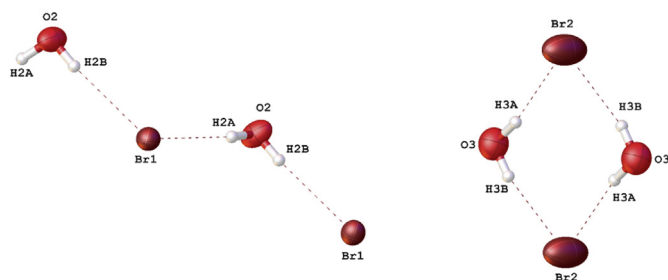
Fig. 10. Hydrogen bonding in the crystal structure of **4**. Thermal ellipsoids are drawn at 50% probability level.

Table 3
Hydrogen bonds in **4** [Å and °].

$D–H\cdots A$	$d(H\cdots A)$	$d(D–H)$	$d(\cdots A)$	$\angle(DHA)$
O2–H2A··· Br1	0.937(16)	2.445(19)	3.347(4)	162(3)
O2–H2B··· Br1[i]	0.842(17)	2.510(16)	3.349(4)	175(5)
O3–H3A···Br2[ii]	0.963(16)	2.356(18)	3.296(4)	165(7)
O3–H3B···Br2[iii]	0.860(17)	2.36(3)	3.141(4)	151(4)

Symmetry transformations used to generate equivalent atoms: (i) x,−y+1/2,z−1/2 (ii) x+1,y,z (iii) −x+1,−y+1,−z.

agreement with work reported by Smith and co-workers [29], who showed that the maximum tolerated acute dosage for a series of phosphonium compounds, in which triphenylphosphonium groups were conjugated to a range of very different molecular entities, were broadly similar.

Rideout et al., and Cheng et al., have previously reported the use of MALDI-TOF-MS to measure the cellular uptake of phosphonium compounds by cancer cell lines. Both studies highlighted the high specificity and sensitivity of the technique for the quantification of phosphonium compounds and the reproducibility of the data. Furthermore, phosphonium compounds have also been used to derivatise proteins [30], and other molecules [31], to improve their detection by mass spectrometry. As well as the difference in cytotoxicity, there is a notable difference in the rate of cellular uptake and level of accumulation of compounds **2** and **4**, the trifluorophenyl derivative being taken-up at lower levels, and at a slower rate than the triphenyl derivative. Similar results were observed by Cheng et al. who found that the 4-fluorophenyl(triphenyl)phosphonium cation [(4-FC$_6$H$_4$)PPh$_3^+$] was taken-up by C6 glioma cells more slowly, and at only 80% of the levels, of the tetraphenylphosphonium cation [Ph$_4$P$^+$].

The poor solubility of the phosphonioalkylthiosulfate zwitterions **1** and **3** was disappointing. A number of different solvents including toluene, THF, methanol, acetone and PBS, cell culture media and β-cyclodextrin, which is widely used in the pharmaceutical industry to enhance drug solubility [32], were investigated. However, none of these proved suitable for dissolving the zwitterions for cell biology experiments. It is interesting to note that phosphonium-functionalised gold nanoparticles derived from zwitterions **1** and **3** are soluble in aqueous media [7]. Cheng et al. observed that (4-carboxybutyl)triphenylphosphonium bromide, which is a zwitterion under physiological conditions, is accumulated only very minimally by cells and was not detectable in MALDI experiments [18]. The poor solubility of **1** and **3** is likely to be linked to the strong non-covalent interactions between adjacent molecules. In addition to electrostatic attractions, **3** displays offset face-to-face phenyl embrace interactions between phenyl rings in adjacent molecules, which are a common feature of the propeller arrangement of phenyl rings in phosphonium and related compound [33], together with intermolecular F···H hydrogen bonding

interactions. These intermolecular interactions serve to stabilise the molecules. The ω-thioacetylpropyl(triaryl)phosphonium salts **2** and **4**, are soluble in a range of solvents. The crystal structure of **4** shows that this compound does not display the phenyl embrace interactions seen in **2**. Furthermore, the F···H hydrogen bonds in **4** are weaker than those in **2** and the complex web of intermolecular interactions in **4** are focused around the bromide anions and waters of crystallisation. This may explain why this compound, and the phenyl analogue **3**, show much greater solubility than the zwitterions.

4. Conclusion

The results show that the ω-thioacetylpropyl(triaryl)phosphonium salts are readily taken-up by cells and can be quantified using MALDI-TOF-MS. The phosphonium salts show low cyctoxicity compared with other triphenylphosphonium compounds, making them potentially useful species for transporting other species, such as metal nanoparticles, into cells. The phosphoniopropylthiosulfate zwitterions are not soluble in aqueous solutions or other solvents which are compatible with biological testing. Crystallographic analysis of the tri(4-fluorophenyl)phosphoniopropylthiosulfate zwitterion (**3**) reveals an extensive array of electrostatic and non-covalent intermolecular interactions which may serve to reduce the solubility of this and related zwitterions in aqueous media.

5. Experimental

5.1. Synthesis of **1** - **4**

Chemicals and solvents were purchased from Sigma-Aldrich or Fisher Scientific Ltd and used as received. All ^{1}H, ^{31}P and ^{19}F NMR spectra were recorded on a Brucker AVANCE III (400 MHz). IR spectra were recorded on a Brucker ALPHA platinum ATR spectrometer. Melting points were determined on a Stuart SMP3 melting point apparatus and are uncorrected. Electrospray Ionisation Mass spectrometry was performed on a Thermo Finnigan LCQ classic in positive ion mode.

The synthesis and spectroscopic data of triphenylphosphoniopropylthiosulfate (**1**) and ω-thioacetylpropyltriphenyl-phosphonium bromide (**2**) have been reported previously [9,10].

Tri(4-fluorophenyl)phosphoniopropylthiosulfate (**3**) and ω-thioacetylpropyl(tri-4-fluorophenyl)phosphonium bromide (**4**) were prepared from (tri-4-fluorophenyl)phosphine as described below:

Tris(4-fluorophenyl)phosphine (1.0 g, 3.16 × 10^{-3} mol) and 3-bromo-1-propanol (1.1 mL, 1.25 × 10^{-2} mol) were refluxed in acetonitrile (20 mL) under nitrogen overnight to yield 3-hydroxypropyl(tri-4-fluorophenyl)phosphonium bromide. Upon completion the reaction mixture was diluted with deionised water (20 mL) and the product isolated by liquid-liquid extraction using dichloromethane (3 × 20 mL). The dichloromethane extracts were combined, dried over MgSO$_4$, and the solvent removed by rotary evaporation. The 3-hydroxypropyl(tri-4-fluorophenyl)phosponium bromide was refluxed with HBr (48%, 10 mL) under nitrogen overnight. Upon completion the reaction mixture was diluted by the addition of deionised water (20 mL) and the product, 3-bromopropyl(tri-4-fluorophenyl)phosphonium bromide, separated by liquid-liquid extraction using dichloromethane (3 × 20 mL). The dichloromethane extracts were combined, dried over MgSO$_4$, and the solvent removed by rotary evaporation, yielding 3-bromopropyl(tri-4-fluorophenyl)phosphonium bromide as a white solid. To produce zwitterion **3**, 3-bromopropyl(tri-4-fluorophenyl)phosphonium bromide (0.250 g, 5.70 × 10^{-4} mol) and Na$_2$S$_2$O$_3$ (0.212 g, 8.56 × 10^{-4} mol) were refluxed in aqueous ethanol. The thioacetate salt **4** was produced by stirring together 3-

bromopropyl(tri-4-fluorophenyl)phosphonium bromide (0.250 g, 5.70×10^{-4} mol) and $KSC(O)CH_3$ (0.098 g, 8.56×10^{-4} mol) in aqueous ethanol. Both compounds were isolated from the reaction mixtures by extraction with dichloromethane (3×20 mL). Purification of the products, which form as white microcrystalline powders, was achieved by triturating with diethyl ether and recrystallising from dichloromethane/diethyl ether. The progress of all of the reactions was monitored by TLC using a mobile phase of 80% dichloromethane: 20% methanol.

Analytical data for compounds **3** and **4** are reported here for the first time:

Tri(4-fluorophenyl)phosphoniopropylthiosulfate **3** M.p. 243 °C; Elemental analysis: found: C, 53.89; H, 3.93; $C_{21}H_{18}F_3O_3PS_2$ requires: C, 53.61; H, 3.86. ^{1}HNMR ($CDCl_3$) = 2.2 (2H, m), 3.3 (2H, m), 3.6 (2H, m), 7.6–8.0 ppm (15H, m). ^{31}P NMR ($CDCl_3$) = 23.3 ppm. ^{19}F NMR ($CDCl_3$) = −99.3 ppm; FT-IR:ν_{max}/cm^{-1} 1209 (S=O). Accurate mass analysis: found 471.0474 [M]$^+$; cation $C_{21}H_{18}F_3O_3PS_2$ requires 433.471.0465[M]$^+$; ω-thioacetylpropyl(tri-4-fluorophenyl)phosphonium bromide **4** M.p. 118 °C; Elemental analysis: found: C, 52.47%; H, 4.09%; $C_{23}H_{21}F_3SOPBr + H_2O$ requires: C, 51.97%; H, 4.33%. ^{1}H NMR ($CDCl_3$) = 1.9 (5H, m), 3.2 (2H, m), 4.3 (2H, m), 7.3–8.1 (12H, m) ppm. ^{31}P NMR ($CDCl_3$) = 23.9 ppm; ^{19}F NMR ($CDCl_3$) = −99.0 ppm; FT-IR:ν_{max}/cm^{-1} 1680 (C=O); Accurate mass analysis: found 433.0976[M]$^+$; cation $C_{23}H_{21}F_3SOPBr$ requires 433.1003[M]$^+$;

5.2. Cell culture

Human prostate cancer cells (PC3) obtained from ATCC were maintained in complete media (cDMEM) which contains Dulbecco's modified Eagle medium with GlutaMAX, 4.5 g/L D-Glucose and sodium pyruvate (Invitrogen Life Technologies, Paisley, Renfrewshire, UK) containing 10% heat-inactivated fetal bovine serum (Biosera, East Sussex, Sussex, UK) and 100 I.U/ml Penicillin and 100u = g/ml Streptomycin (Invitrogen Life Technologies Paisley, Renfrewshire, UK) at 37 °C in 5% CO_2 and 95% air. Cells were subcultured every 3 days and routinely screened for *Mycoplasma Spp.*

5.3. Cytotoxicity assay

Cytotoxicity was assessed using CellTiter-Glo™ luminescent cell viability assay kit (Promega Corporation, Southampton, Hampshire, UK). PC3 cells were seeded in opaque-walled 96-well plates at a density of 10,000 cells/well and allowed to adhere overnight. Cells were subsequently treated with the corresponding phosphonium compound (0−1000 μM) for 24, 48 and 72 h. After each incubation period cell viability was measured according to the manufacturer's instructions; plates were equilibrated at room temperature for 30 min, 100 μL of assay reagent was added to each well, placed on an orbital shaker for 2 min, left to stand at room temperature for 10 min and read on a Wallac Victor2 1420 multilabel counter (PerkinElmer, Cambridge, Cambridgeshire, UK). All measurements were performed in quadruplicate, 3 independent experiments were conducted (n = 12). All plates contained the following control wells: control 1 - cells plus cDMEM only, control 2 - cells plus cDMEM with 0.1% DMSO, control 3 − cells plus cDMEM with 0.01% DMSO and control 4 - cells plus cDMEM with 0.001% DMSO. Data are expressed as a percentage of live cells normalised to control, the average, standard deviation and IC_{50} values were plotted and calculated using GraphPad Prism (GraphPad software, La Jolla, California, USA).

5.4. Cellular uptake studies of phosphonium compounds by MALDI-MS

Matrix-assisted laser desorption ionisation mass spectrometry (MALDI-MS) and laser desorption ionisation mass spectrometry (LDI-MS) experiments were performed in positive ion mode on an applied Biosystems/MDS Sciex hybrid quadrupole time-of-flight mass spectrometer (Q-Star Pulsar-*i*) with an orthogonal MALDI ion source (Applied Biosystems, Foster City, California, USA) and a high repetition Neodymium-doped yttrium vandate (Nd: YVO_4 laser (5 KHz)) (Elforlight Ltd, Daventry, Northamptonshire, UK). Spectra were collected with an acquisition time of 1 min. Uptake studies of phosphonium compounds by MALDI were conducted using the method reported previously by Cheng et al.[18].

5.5. Calibration curve of phosphonium compounds for semi-quantification analysis by MALDI-MS

PC3 cells were cultured in T75 flasks; after trypsinsation, the cells were washed twice with PBS (Invitrogen Life Technologies, Paisley, Renfrewshire, UK), re-suspended in deionised H_2O to lyse the cells and aliquoted at a density of 3.5×10^6 cells/mL. Phosphonium compounds and internal standards were dissolved in methanol and diluted with PC3 cell lysate to make various concentrations and stored at 4 °C. 10 μL of phosphonium compound and 10 μL of internal standard were mixed thoroughly; sequentially 10 μL of this solution was mixed with 10 μL of matrix (DHB or α-CHCA) and 0.5 μL of sample was deposited on the target MALDI plate. MALDI matrices (DHB or α-CHCA) were made to a concentration of 10 mg/mL in 70:30 acetonitrile:water with 0.1% tetrafluoroacetic acid. Triplicate standards were prepared and analysed; standards collected from 3 independent cell lysates were prepared for each study.

5.6. Sample preparation of phosphonium compounds for semi-quantification analysis by MALDI-MS

PC3 cells were cultured in T75 flasks; after trypsinsation, the cells were washed with PBS twice, re-suspended in low K$^+$ HEPES buffer (NaCl, 135 mM, KCl 5 mM, $CaCl_2$ 1.8 mM, $MgSO_4$ mM, HEPES 50 mM, dextrose 5.5 mM, pH 7.4) and aliquoted at a density of 10×10^6 cells/mL. For cellular uptake studies, PC3 cells (0.5×10^6 cells/50 μL) were incubated with 10 μL of 100 μM stock solution of corresponding phosphonium salt (final concentration, 5 μM) and 140 μL of low K$^+$ HEPES buffer and incubated between 0 and 120 min at 37 °C. Subsequent to each incubation period, cells were centrifuged ($500 \times g$, 4 min) and washed twice in cold PBS. Cell pellets were then lysed with 150 μL of cold DIH_2O and placed on dry ice. Prior to MALDI analysis, samples were thawed and centrifuged ($12,000 \times g$, 5 min). The sample cell lysate (90 μL) and 10 μM (10 μL) of the internal standard were mixed together, subsequently 10 μL of this solution was mixed with 10 μL of matrix and 0.5 μL of sample was deposited on the target MALDI plate. Triplicate samples were prepared and analysed, samples collected from 3 independent cell lysates were prepared for each study.

6. X-ray crystallography

X-Ray crystallographic data of **3** and **4** were collected on a Bruker APEXII CCD diffractometer mounted at the window of a Bruker FR591 rotating anode (MoKα, λ = 0.71,073 Å) and equipped with an Oxford Cryosystems Cryostream device. Data were processed using the COLLECT package [34] and unit cell parameters were refined against all data. An empirical absorption correction was carried out using SADABS [35]. Crystal structure was solved by

direct methods using SHELXS-97 and refined on F_o^2 by full-matrix least-squares refinements using SHELXL-97 (**3**) and SHELXL-2014 (**4**) [36].

All non-hydrogen atoms were refined with anisotropic displacement parameters. All hydrogen atoms were added at calculated positions and refined using a riding model with isotropic displacement parameters based on the equivalent isotropic displacement parameter (U_{eq}) of the parent atom, except those on O2 and O3 in **4**, where DFIX and DANG restraints were used to maintain appropriate geometry.

In the crystal structure of **3**, the $-SO_3$ group is disordered over two positions with approximately 88:12 ratio (the minor component is refined isotropically). In the crystal structure of **4**, the $-CH_2SCOCH_3$ group is disordered over two sites with approximately 91:09 ratio with SIMU, DELU and RIGU restraints applied to the disordered atoms. Graphics were generated using OLEX2 [37] and MERCURY [38]. The corresponding CIF has been deposited with the Cambridge Crystallographic Data Centre.

Crystallographic data of **3**: a = 9.4169(13), Å, b = 15.279(3) Å, c = 16.090(3) Å, α = 73.281(7)°, β = 77.619(10) °, γ = 73.052(9)°; V = 2099.2(6) Å^3, triclinic, *P*-1, Z = 4, (Z' = 2), ρ_{calc} = 1.489 Mg/m^3; μ = 0.377 mm^{-1}; T = 120(2) K; θ_{max} = 27.48°, 40,825 measured reflections, 9403 unique reflections [R_{int} = 0.1243], 4672 with $F^2 > 2\sigma$, R(F, $F^2 > 2\sigma$) = 0.0830; R_w(F^2, all data) = 0.2039, GoF = 1.035, CCDC: 1,474,049.

Crystallographic data of **4**: a = 14.8827(3) Å, b = 31.9320(5) Å, c = 10.6385(2) Å, α = 90°, β = 108.9170(10)°, γ = 90°; V = 4782.71(15) Å^3, Monoclinic, *P*2$_1$/*c*, Z = 8, ρ_{calc} = 1.476 Mg/m^3; μ = 1.914 mm^{-1}; T = 120(2) K; θ_{max} = 25.00°, 78,770 measured reflections, 8401 unique reflections [R_{int} = 0.0811], 6738 with $F^2 > 2\sigma$, R(F, $F^2 > 2\sigma$) = 0.0727; R_w(F^2, all data) = 0.2018, GoF = 1.031, CCDC: 1,474,050.

Acknowledgements

Appendix A. Supplementary data

Supplementary data related to this article can be found at http://dx.doi.org/10.1016/j.ejmech.2016.08.025.

References

[1] M.F. Ross, G.F. Kelso, F.H. Blackie, A.M. James, H.M. Cocheme, A. Filipovska, T. Da Ros, T. R. Hurdy, R.A.J. Smith, M.P. Murphy, Biochem. Mosc. 70 (2005) 222.
[2] (a) V. Weissig, Pharm. Res. 28 (2011) 2657–2668;
(b) A.T. Hoyle, J.E. Davoren, P. Wipf, M.P. Fink, V.E. Kagan, Acc. Chem. Res. 41 (2008) 87–97.
[3] (a) Z. Liu, C. Zhang, Y. Chen, W. He, Z. Guo, Chem. Commun. 48 (2012) 8365–8367;
(b) M. Li, G.M. Gnea, C. Lu, S.L. De Rooy, B. El-Zahab, V.E. Ferand, R. Jin, S. Aggarwal, I.M. Warner, J. Inorg. Biochem. 107 (2012) 40–46;
(c) C.-K. Koo, LK.-Y. So, K.-L. Wong, Y.-M. Ho, Y.-W. Lam, M.H.-W. Lam, K.-W. Cheah, C.C.-W. Cheng, W.-M. Kwok, Chem. Eur. J. 16 (2010) 3942–3950;
(d) Y.-S. Kim, C.-T. Yang, J. Wang, L. Wang, Z.-B. Li, X. Chen, S. Liu, J. Med. Chem. 51 (2008) 2971–2984;
(e) C.-T. Yang, Y. Li, S. Liu, Inorg. Chem. 46 (2007) 8988–8997.
[4] S. Biswas, N.S. Dodwadkar, A. Piroyan, V.P. Torchilin, Biomaterials 33 (2012) 4773–4782.
[5] (a) S.V. Boddapati, G.G.M. D'Souza, S. Erdogan, V.P. Torchilin, V. Weissig, Nano Lett. 8 (2008) 2559–2563;
(b) S. Biswas, N.S. Dodwadkar, P.P. Deshpande, V.P. Torchilin, J. Control.
Release 159 (2012) 393–402;
(c) S.V. Boddapati, P. Tongcharoensirikul, R.N. Hanson, G.G.M. D'Souza, V.P. Torchilin, V. Weissig, J. Liposome Res. 15 (2005) 49–58.
[6] (a) Y. Zhang, Y. Shen, X. Teng, M. Yan, H. Bi, P.C. Morais, ACS Appl. Mater. Interfaces 7 (2015) 10201–10212;
(b) M.N. Tahir, R. Ragg, F. Natalio, J.K. Sahoo, P. Daniel, K. Koynov, D. Strand, S. Strand, W. Tremel, J. Mater. Chem. B 3 (2015) 2371–2377;
(c) G.-F. Luo, W.-H. Chen, Y. Liu, Q. Lei, R.-X. Zhuo, X.-Z. Zhang, Sci. Rep. 4 (6064) (2014) 1–9;
(d) X.-H. Wang, H.-S. Peng, L. Yang, F.-T. You, F. Teng, L.-L. Hou, O. Wolfbeis, Angew. Chem. Int. Ed. 53 (2014) 12471–12475;
(e) X.-H. Wang, H.-S. Peng, L. Yang, F.-T. You, F. Teng, A.-W. Tang, F.-J. Zhang, X.-H. Li, J. Mater. Chem. B 1 (2013) 5143–5152.
[7] Y. Ju-Nam, Y.-S. Chen, J.J. Ojeda, D.W. Allen, N.A. Cross, P.H.E. Gardiner, N. Bricklebank, RSC Adv. 2 (2012) 10345–10351.
[8] Y. Yang, N. Gao, Y. Hu, C. Jia, T. Chou, H. Du, H. Wang, Ther. Deliv. 6 (2015) 307–321.
[9] Y. Ju-Nam, N. Bricklebank, D.W. Allen, P.H.E. Gardiner, M.E. Light, M.B. Hursthsuse, Organic and Biomol. Chem. 4 (2006) 4345–4351.
[10] (a) Y. Ju-Nam, D.W. Allen, P.H.E. Gardiner, N. Bricklebank, J. Organomet. Chem. 693 (2008) 3504–3508;
(b) Y. Ju-Nam, D.W. Allen, P.H.E. Gardiner, N. Bricklebank, M.E. Light, M.B. Hursthouse, J. Organomet. Chem. 692 (2007) 5065–5070.
[11] Y.-S. Chen, Sheffield Hallam University, PhD Thesis, 2014.
[12] M.F. Ross, T.A. Prime, I. Abakumova, A.M. James, C.M. Porteous, R.A.J. Smith, M.P. Murphy, Biochem. J. 411 (2008) 633–645.
[13] (a) H.J. Böhm, D. Banner, S. Bendels, M. Kansy, B.M. Kuhn, K. Ller, U. Obst-Sander, M. M. Stahl, ChemBioChem 5 (2004) 637–643;
(b) R. Filler, R. Saha, Future Med. Chem. 1 (2009) 777–791.
[14] (a) see for example H. Zheng, X. Wu, F. Song, C. Xu, H. Liu, W. Liu, Eur. J. Med. Chem. 118 (2016) 90–97;
(b) A. Haslop, L. Wells, A. Gee, C. Plisson, N. Long, Mol. Pharm. 11 (2014) 3818–3822;
(c) Z. Zhao, Q. Yu, T. Mou, C. Liu, W. Yang, W. Fang, C. Peng, J. Lu, Y. Liu, X. Zhang, Mol. Pharm. 11 (2014) 3823–3831.
[15] M. Millard, D. Pathania, Y. Shabaik, L. Taheri, J. Deng, N. Neamati, PLoS One 5 (2010) e13131.
[16] L.H. Cohen, A.I. Gusev, Anal. Bioanal. Chem. 373 (2002) 571–586.
[17] D. Rideout, A. Bustamante, G. Siuzdak, Proc. Natl. Acad. Sci. 90 (1993) 10226–10229.
[18] Z. Cheng, R.C. Winant, S.G. Gambhir, J. Nucl. Med. 46 (2005) 878–886.
[19] J.-X. Chen, Q.-F. Xu, Y. Zhang, S.M. Zain, S.W. Ng, P.-P. Lang, Acta. Cryst. Sect. C C60 (2004) 0572–0574.
[20] N. Lalwani, Y.-S. Chen, G. Brooke, N.A. Cross, D.W. Allen, A. Reynolds, J. Ojeda, G.J. Tizzard, S.J. Coles, N. Bricklebank, Chem. Commun. 51 (2015) 4109–4111.
[21] O.B. Shawkataly, J. Singh, K. Sivakumaraaa, H.-K. Fun, Acta. Cryst., Sect. C C52 (2004) 2243–2245.
[22] J.E. Huheey, Inorganic Chemistry : Principles of Structure and Reactivity, Harper Row, New York, 1972.
[23] K. Miaskiewicz, R. Steudel, Angew. Chem. Int. Edn. 31 (1992) 58–59.
[24] C.A. Hunter, J.K.M. Sanders, J. Am. Chem. Soc. 112 (1990) 5525–5534.
[25] F. Cozzi, R. Annunziata, M. Benaglia, K.K. Baldridge, G. Aguirre, J. Estrada, Y. Sritana-Anant, J.S. Siegel, Phys. Chem. Chem. Phys. 10 (2008) 2686–2694.
[26] J.D. Dunitz, R. Taylor, Chem. Eur. J. 3 (1997) 89–98.
[27] K. Reichenbacher, H.I. Suss, J. Hulliger, Chem. Soc. Rev. 34 (2005) 22–30.
[28] M.F. Erben, R. Boese, C.O. Della V Dova, H. Oberhammer, H. Willner, J. Org. Chem. 71 (2006) 616–622.
[29] R.A.J. Smith, R.C. Hartley, H.M. Cochem, M.P. Murphy, Trends Pharmacol. Sci. 33 (2012) 341–352.
[30] Z.-H. Huang, J. Wu, K.D.W. Roth, Y. Yang, D.A. Gage, J.T. Watson, Anal. Chem. 69 (1997) 137–144.
[31] S.J. Barry, R.M. Carr, S.J. Lane, W.J. Leavens, C.O. Manning, S. Monté, I. Waterhouse, Rapid Commun. Mass Spec. 17 (2003) 484–497.
[32] T. Loftsson, M.E. Brewster, J. Pharm. Sci. 85 (1996) 1017–1025.
[33] I. Dance, M. Scudder, Cryst. Eng. Commun. 11 (2009) 2233–2247.
[34] R. Hooft, Collect: Data Collection Software, Nonius B. V., Delft, The Netherlands, 1998.
[35] G.M. Sheldrick, SADABS. Version 2007/2, Bruker AXS Inc, Madison, Wisconsin, USA, 2007.
[36] G.M. Sheldrick, Acta Crystallogr. Sect. A Found. Crystallogr. 64 (2008) 112–122.
[37] O.V. Dolomanov, L.J. Bourhis, R.J. Gildea, J.A.K. Howard, H. Puschmann, J. Appl. Cryst. 42 (2009) 339–341.
[38] C.F. Macrae, I.J. Bruno, J.A. Chisholm, P.R. Edgington, P. McCabe, E. Pidcock, L. Rodriguez-Monge, R. Taylor, J. van de Streek, P.A. Wood, Mercury csd 2.0-New features for the visualization and investigation of crystal structures, J. Appl. Cryst. 41 (2008) 466–470.